agronomy

MDPI

Article

Plant Defence Induction by *Meyerozyma guilliermondii* in *Vitis vinifera* L.

José María Alonso de Robador [1], Nora Ortega Pérez [1], M. Teresa Sanchez-Ballesta [2], M. Luisa Tello Mariscal [3], Beatriz Pintos López [1] and Arancha Gómez-Garay [1,*]

[1] Research Group FiVe-A, Plant Physiology Unit, Genetic, Physiology and Microbiology Department, Faculty of Biological Sciences, Universidad Complutense de Madrid, Ciudad Universitaria, E-28040 Madrid, Spain; jalonsod@ucm.es (J.M.A.d.R.); noortega@ucm.es (N.O.P.); bpintos@ucm.es (B.P.L.)
[2] Department of Characterization, Quality and Safety, Institute of Food Science, Technology and Nutrition (ICTAN-CSIC), Ciudad Universitaria, E-28040 Madrid, Spain; mballesta@ictan.csic.es
[3] INIA-CSIC, Ministry of Science and Innovation, Carretera de la Coruña Km 7.5, E-28040 Madrid, Spain; marisa.tello@inia.csic.es
* Correspondence: magom02@ucm.es

Abstract: This article emphasizes the crucial importance of yeast *Meyerozyma guilliermondii* (Patent CECT13190) as a biological control agent (BCA) in eliciting defensive responses in vine plants, and is supported by comprehensive physiological, proteomic, and transcriptomic analyses. The results demonstrate that the BCA *M. guilliermondii* can induce enhanced defensive responses, as reflected in the regulation of key proteins. Notably, the upregulated expression of calmodulin and pathogenesis-related protein 10 (PR-10) are indicative of a complex interplay between calcium signalling, salicylic acid accumulation, and the elicitation of plant defence responses against pathogens. Furthermore, changes in microtubule dynamics and proteins related to protein synthesis and folding are observed, confirming the elicitation of defence responses. The correspondence between proteomic and transcriptomic analyses for genes codifying pathogenesis-related proteins, such as Vcgns1, VviTL1, and Vcchit1b, reinforces the empirical robustness of our findings. Collectively, our research explores the modulation of plant defences by the BCA, opening promising avenues for innovative agricultural strategies that enhance crop resilience and productivity.

Keywords: biocontrol; yeast; vine; *Fusarium equiseti*; gene expression; proteomic analysis

Citation: Alonso de Robador, J.M.; Ortega Pérez, N.; Sanchez-Ballesta, M.T.; Tello Mariscal, M.L.; Pintos López, B.; Gómez-Garay, A. Plant Defence Induction by *Meyerozyma guilliermondii* in *Vitis vinifera* L. *Agronomy* **2023**, *13*, 2780. https://doi.org/10.3390/agronomy13112780

Academic Editor: Gianluca Allegro

Received: 30 September 2023
Revised: 30 October 2023
Accepted: 1 November 2023
Published: 8 November 2023

1. Introduction

Vitis vinifera, commonly known as grapevine, holds significant economic importance in Spain as a source of table grapes and wine production. However, grapevine cultivation faces various challenges, including the emergence of wood diseases. In recent years, wood diseases have witnessed a considerable increase due to factors such as the expansion of vineyard areas since the 1990s, changes in production methods (e.g., trellising systems, mechanical pruning), and the abandonment of certain fungicides (e.g., sodium arsenite, benzimidazole) due to environmental and public health concerns [1].

One notable pathogen that has become a concern in grapevine cultivation is *Fusarium equiseti*. In 2019, the first infection of *Vitis vinifera* by *Fusarium equiseti* was reported in Spain, posing a new risk to grape cultivation [2]. This pathogen, detected in nurseries, has raised alarm within the grape industry. *Fusarium equiseti* represents a significant threat due to its potential to cause wood diseases in grapevines. As a result, identifying effective biocontrol measures against *Fusarium equiseti* has become a fundamental objective in safeguarding the production of this globally and nationally important crop. In this study, we specifically investigated the inducing effect of treatments against *Fusarium equiseti*, aiming to develop biocontrol strategies to protect the crop from this pathogenic fungus.

In addition to controlling pathogenic infections, understanding the impact of biocontrol agents (BCAs) and their interactions with grapevines is crucial. BCAs, such as *Meyerozyma guilliermondii*, have shown promise in mitigating abiotic stress effects, enhancing stress tolerance, and improving crop performance [3]. *Meyerozyma guilliermondii*, well-known for its antagonistic effects against postharvest diseases in pears and its ability to degrade patulin [4], represents a promising biological control agent. It is noteworthy that other species within the *Meyerozyma*/*Pichia* genus have been recognized as BCAs effective against post-harvest biotic diseases [5]. In our study, *M. guilliermondii* demonstrates its efficacy as a pre-harvest BCA, exhibiting control activity against the pathogenic fungus *Fusarium equiseti* in *Vitis vinifera* L. These BCAs establish mutualistic relationships with grapevines and offer various benefits, including the ability to withstand biotic and abiotic stresses, such as excessive temperature, drought, or salinity, enhancing nutrient acquisition, and increasing yield [6].

In order to fully evaluate the effects of BCAs, it is essential to analyse various aspects of grapevine physiology and defence mechanisms. In this study, we investigated the impacts of different treatments, including pathogen infection, BCA inoculation, and the sequential inoculation of the pathogen and BCA, on the growth-related morphological characteristics, oxalic acid content, salicylic acid content, and superoxide dismutase (SOD) activity in *Vitis vinifera*. Additionally, we conducted proteomic analysis and gene expression studies targeting pathogenesis-related β-1,3-glucanase (also called β-1,3-glucosidase), thaumatin, and chitinase genes.

By comprehensively investigating these factors, including morphological characteristics, oxalic acid content, salicylic acid content, SOD activity, proteomic profiles, and gene expression patterns, we aim to gain a deeper understanding of the effects of different treatments on *Vitis vinifera*. This knowledge will contribute to the development of sustainable and effective strategies for grapevine protection and cultivation.

2. Materials and Methods

2.1. The Microorganisms Used in this Study

In this study, two microorganisms were used: *Meyerozyma guilliermondii* (Patent CECT13190) and *Fusarium equiseti*. *M. guilliermondii* is a beneficial yeast known for its potential in mitigating abiotic stress effects and enhancing crop performance. On the other hand, *F. equiseti* is a pathogenic fungus that poses a risk to *Vitis vinifera* [2]. By including both microorganisms in the experimental setup, it was possible to evaluate their contrasting effects on plant health and growth.

2.2. Plant Material and Experimental Setup

2.2.1. Plant Material

For the biocontrol experiments in *Vitis vinifera* L., 72 glass jars (17 × 25.5 × 7 cm) were used. These jars were thoroughly washed with soap, bleach, and distilled water prior to use. They were then filled with vermiculite and sterilized in an autoclave at 121 °C for 20 min.

The plant material: 72 grafted grapevine plants (certified Tempranillo clone RJ51/110R-E35) that had rooted were immersed in 70% ethanol for 5 min, followed by a 4% bleach solution for 10 min. Finally, the cuttings were rinsed three times in autoclaved distilled water, with each rinse lasting 5 min.

The grafted grapevine plants were placed in the glass jars with vermiculite, ensuring that the roots were covered. In this study, controlled experimental conditions were established at a constant temperature of 20 ± 2 °C, with a light cycle of 16 h of light and 8 h of darkness. The grafted grapevine plants were watered with filtered water to maintain moisture in the vermiculite. Additionally, once a week, they were irrigated with a 1:10 dilution of Hoagland No. 2 nutrient solution [7]. The solution contained macronutrients including nitrogen (N) at 14 mM, phosphorus (P) at 1 mM, potassium (K) at 5 mM, calcium (Ca) at 4 mM, magnesium (Mg) at 2 mM, and sulphur (S) at 2 mM. Additionally, micronutrients

such as iron (Fe) at 20 µM, manganese (Mn) at 2 µM, zinc (Zn) at 2 µM, copper (Cu) at 0.5 µM, molybdenum (Mo) at 0.1 µM, and boron (B) at 25 µM were included in the solution. Data on phenology were recorded after the bud break.

The phenological status of each individual grafted grapevine plant (vine) was monitored throughout the experiment, following the phenological scale proposed by Baggiolini [8]. Once the plants reached the phenological stage "E" (extended leaves), the inoculation treatments were conducted.

2.2.2. Experimental Design and Treatments

The experimental trial with the microorganisms began when the vines had fully developed leaves and tendrils. All the vines were at phenological stage E ("extended leaves"). Each biological replicate corresponds to a pool of three plants, with three biological replicates per treatment. Therefore, a total of nine plants were included in each treatment group, distributed across three biological replicates. Additionally, the experiment was replicated twice, providing two repetitions of the entire study. Three groups were randomly formed for the inoculation experiments, consisting of selected vines:

Group 1: Control—vines were watered with filtered tap water.

Group 2: BCA Inoculation—inoculation with yeast solution (4 mL of PDB medium containing yeast grown for 48 h at 120 rpm agitation; approx. 8×10^8 CFU/mL).

Group 3: Pathogen Inoculation—inoculation with *Fusarium equiseti*. Three PDA plates with the fungus grown on the entire surface were used. The agar with mycelium was placed in a container with 300 mL of autoclaved distilled water and then chopped to release spores and mycelium. After inoculation, all the vines were watered with filtered water for 20 days.

Each plant received a specific volume in its individual pot or container. The exact volume used for inoculation was 25 mL for each plant or pot. This method ensured uniform distribution and contact with the plant's root system.

Two weeks after the first inoculation, a second inoculation was performed. From the 18 vines in each trial, from Group 2 (yeast-inoculated) and Group 3 (fungus-inoculated), 9 vines were inoculated with the fungus or yeast, as appropriate. The subdivision of vines in each group was performed completely at random. Therefore, the assays were as follows:

Group 1 (C): Control—vines were watered with filtered tap water.

Group 2a (BCA): Yeast Inoculation—inoculation with a yeast solution.

Group 2b (BCA + P): Yeast + pathogen—vines initially inoculated with yeast were subsequently inoculated with *F. equiseti* after 20 days of the initial trial. The inoculation of the fungal pathogen was carried out in the same manner as in the other trials.

Group 3a (P): Pathogen Inoculation—inoculation with *F. equiseti*.

Group 3b (P + BCA): Pathogen + Yeast—vines initially inoculated with *F. equiseti* were subsequently inoculated with yeast after 20 days of the initial trial. The inoculation of yeast was carried out in the same manner as in the other trials.

The entire experiment was replicated twice, with each treatment consisting of three groups of three plants.

2.3. Disease Symptoms and Physiological Parameters

2.3.1. Symptomatology

In our study evaluating the disease incidence in *Vitis vinifera* plants, we conducted direct observations focusing on symptoms associated with *Fusarium* wilt. The key manifestation of this disease is the abrupt wilting of leaves, typically beginning from the lower leaves and advancing upwards. This wilting can either be transient, transpiring during the hottest periods of the day, or it can progress into a permanent condition, ultimately leading to the death of the plant. Four weeks after the two rounds of inoculation, we gathered symptom data from vine shoots, recording the count of healthy, diseased, and deceased shoots within each of the experimental groups.

2.3.2. Determination of Salicylic Acid in Leaves

To determine the in situ salicylic acid in leaves, the protocol described by Tseng et al. [9] was followed. From plants belonging to C, P, and BCA assays, the apical leaves of each vine shoot were collected, submerged in a TiO_2 nanoparticles solution, and agitated at 120 rpm for 24 h. After that time, photos of each leaf were taken to subsequently assess the area of brown spots corresponding to salicylic acid production in the leaves. The areas were measured using the ImageJ® software, version 1.8.0.

2.3.3. SOD Activity Assay

To assess the production of SOD, the protocol described by Beauchamp and Fridovich [10] was followed. Plant tissue weighing 250 mg was taken from each inoculation assay, and the samples were then treated with liquid nitrogen and ground using an electric grinder (IKA, A 10 basic). The measurements were performed in triplicate for each sample.

2.3.4. Oxalic Acid Assay

An evaluation of oxalic acid production was conducted in the different vine shoot assays. For this purpose, the Oxalic Acid Colorimetric Assay Kit MAK179-1KT (Sigma Aldrich, Saint Louis, MI, USA) was used. A total of 250 mg of plant tissue (in triplicate) from each inoculation treatment was taken, having been treated with liquid nitrogen and an electric grinder.

2.4. Proteomic Analysis

2.4.1. Sample Preparation

Each biological replicate corresponds to a pool of three plants, with three biological replicates per treatment. TCA/Acetone-precipitated samples were analysed in duplicate. The samples were resuspended in 40 µL of 100 mM TEAB (riethyl ammonium bicarbonate) buffer. Protein quantification was performed using fluorimetry on the Qubit fluorometer (Thermo Fisher Scientific, Waltham, MA, USA).

2.4.2. Tryptic Digestion in Solution

For this purpose, the samples were reduced with 10 mM DTT at 37 °C for 60 min, followed by alkylation with 25 mM Iodoacetamide in darkness for 60 min. Subsequently, 0.25 µg of recombinant sequencing-grade trypsin (Roche Molecular Biochemicals, Basel, Switzerland) in 25 mM ammonium bicarbonate (pH 8.5) was added to each sample, and the mixture was incubated overnight at 37 °C. The peptides resulting from digestion were dried via vacuum centrifugation (SpeedVac, Thermo Scientific, Bremen, Germany) and reconstituted in 12 µL of 2% ACN, 0.1% Formic Acid (FA) solution. The samples were then frozen at −20 °C until LC-MS/MS analysis.

2.4.3. LC-MS/MS Analysis

The peptides were analysed via nano-liquid chromatography (nano Easy-nLC 1000, Thermo Scientific, MA, USA) coupled to a Q-Exactive HF high-resolution mass spectrometer (Thermo Scientific, Bremen, Germany). The peptides were concentrated online via reverse-phase chromatography (RP) using an Acclaim PepMap 100 pre-column (Thermo Scientific, Bremen, Germany) (20 mm × 75 µm ID, 3 µm particle size, and 100 Å pore size), and then separated on a C18 Picofrit column (Thermo Scientific Easy Spray Column, PepMap RSLC C18n, Bremen, Germany) (500 mm × 75 µm ID, 2 µm particle size, and 100 Å pore size) with an integrated spray tip, operating at a flow rate of 250 nL/min. Peptides were eluted using a gradient from 2% to 35% of buffer B over 150 min, followed by an increase from 35% to 45% buffer B over 10 min (Buffer A: 0.1% FA in water; Buffer B: 0.1% FA in ACN).

The nano-HPLC was online coupled to the Easy nanoelectrospray source of the Q-Exactive HF mass spectrometer for peptide analysis. Peptides were introduced via ionization with electrospray, using the integrated tip in the analytical column.

Data acquisition was performed with a spray voltage of 1.7 kV for electrospray, and the ion transfer tube guiding ions from the spray to the interior of the mass spectrometer was maintained at a temperature of 290 °C. A data-dependent acquisition (DDA) method was used to detect peptides in the samples. In this method, peptides were detected in Full scan MS mode with a resolution of 60,000 over a mass range of m/z 350–1800 Da. MS/MS data were acquired in data-dependent mode (DDA) with a resolution of 30,000. Up to 15 precursor ions with charge states from 2+ to 4+ were selected per micro-scan based on their intensity (threshold: 1×10^4), with a dynamic exclusion of 10 s. The selected precursors were isolated with a window width of ± 2 m/z units and fragmented via High Collision Dissociation (HCD) with a normalized collision energy of 20%. MS/MS spectra were acquired in positive mode.

2.4.4. Protein Identification

The data were analysed using Proteome Discoverer 2.4 software (Thermo Scientific) with the Mascot 2.6 search engine (matrixscience.com, accessed on 4 May 2022). The following databases were used:

- UP-*Vitis vinifera* (160,461 sequences), downloaded from Uniprot (https://www.uniprot.org, accessed on 4 May 2022).
- UP-*Meyerozyma guilliermondii* (5974 sequences), downloaded from UniProt.
- UP-*Fusarium equiseti* (338 sequences), downloaded from Uniprot, and
- NCBI-*Fusarium equiseti* (382 sequences), downloaded from NCBI.

The following parameters were used in the Mascot searches for peptide identification: a peptide precursor tolerance of 10 ppm, a fragment tolerance of 0.02 Da, up to two missed cleavages for trypsin, carbamidomethyl cysteine as a fixed modification, and oxidation of methionine and N-terminal acetylation as variable modifications.

Proteins were considered "correctly" identified if they met the following criteria: a False Discovery Rate (FDR) below 1% and at least one uniquely identified peptide with a Confidence Interval (CI) exceeding 99%. This means that the probability of the identified peptide being a result of random chance is less than 1% (q-value < 0.01).

2.4.5. Protein Annotation and Functional Analysis

The identified proteins were subjected to functional analysis using the Database for Annotation, Visualization, and Integrated Discovery (DAVID, http://david.abcc.ncifcrf.gov/, accessed on 4 May 2022; Sherman et al., 2022 [9]). Gene Ontology (GO) and Kyoto Encyclopaedia of Genes and Genomes (KEGG) analyses were performed to gain insights into the biological processes and pathways associated with the identified proteins. The Protein–Protein Interaction (PPI) network was analysed using the STRING database v11.5 (https://string-db.org/, accessed on 4 May 2022) by predicting functional associations between different proteins based on their known interactions. A minimum required p-value < 0.05 was selected as a threshold for high-confidence results.

2.5. Gene Expression Analysis

2.5.1. Extraction, Purification, and Quantification of Total RNA and Complementary DNA (cDNA) Synthesis

To evaluate the expression of different genes encoding pathogenesis-related proteins (*PRs*) total RNA extraction was performed. For this purpose, leaves from the different grapevines used in this study were frozen in liquid nitrogen and ground using an electric grinder.

Total RNA was extracted three times from each sample according [10] and treated 220 with DNase I recombinant-RNase free (Invitrogen, TM, USA) for genomic DNA removal. The 221 purity and concentration of the extracted RNA from each sample were quantified using a 222 Nanodrop ND-100 spectrophotometer (NanoDrop® Technologies, Wilmington, NC, USA). Then, 1 µg of each ex-223 traction was used to synthesize cDNA

via the NZY FirstStrand cDNA Synthesis kit 224 (NZYtech, Lisboa, Portugal), according to the manufacturer's instructions.

2.5.2. Relative Gene Expression via Real-Time Quantitative PCR (RT-qPCR)

The relative expression of genes encoding thaumatin (*VviTL1*) (AF003007), class I chitinase (*Vcchit1b*) (DQ267094), and class I β-1,3-glucanase (*Vcgns1*) (DQ267748), was performed using RT-qPCR. Oligonucleotides designed by Romero et al. [11,12] were used.

The expression was quantified using NZY qPCR Green Master Mix (NZYtech, Lisbon, Portugal) according to the manufacturer's specifications. Amplifications were run in a 96-well-plates iCycler iQ thermal cycler (Bio-Rad, Hercules, CA, USA) and the results were processed using the iCycler iQTM associ-ated software (Real Time Detection System Software, version 2.0).

Three biological replicates, with two technical replicates each, were performed for each sample and each gene. The grapevine ubiquitin gene (EE253706) was used as an internal reference gene to normalize the amplification values. The relative gene expression was estimated via the $2^{-\Delta\Delta Ct}$ method [13], relative to the control reference sample (C). The specificity of products was validated in accordance with Romero et al. [11].

2.6. Statistical Analysis

The statistical analysis was performed using the STATISTICA® software, Version 8. A one-way analysis of variance (ANOVA) was conducted to compare the means of the different treatment variables. Duncan's test was applied to display the grouping and differences among treatments.

3. Results

3.1. Disease Symptoms

The results of the experiment are summarized in Figure 1, which shows the number of healthy, diseased, and dead plants for each treatment group. After inoculation with *F. equiseti*, a significant number of plants showed symptoms of the disease. In the yeast treatment group, all plants remained healthy throughout the experiment, showing no signs of disease or mortality. In the preventive treatment group, 45% of the plants remained healthy, while 33% showed symptoms of disease, and 22% died. In the curative treatment group, a high percentage of plants (89%) remained healthy, with no incidence of the disease. However, a small proportion (11%) of the plants in this group died.

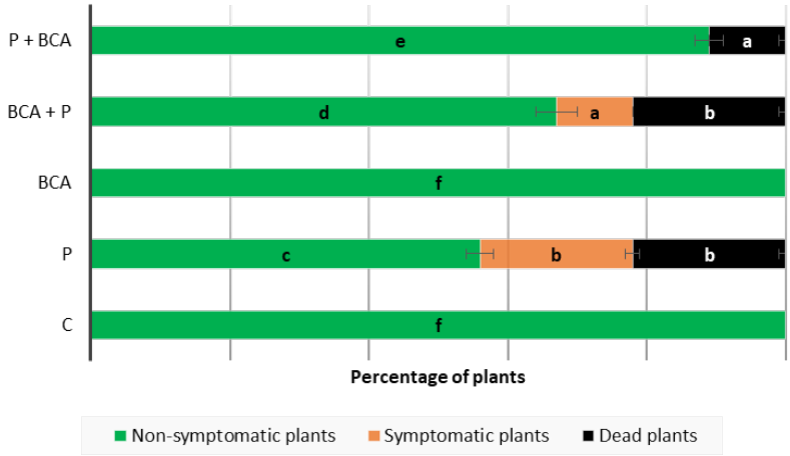

Figure 1. Disease incidence and mortality rates in different treatment groups. It is possible to distinguish between the treatments: Control (C), plants inoculated with *M. guilliermondii* (BCA), plants inoculated with *F. equiseti* (P), and those subjected to a dual inoculation; BCA + P, and P + BCA. Different letters accompanying the data in the figure denote statistically distinct groups ($p \leq 0.05$) via Duncan's test.

3.2. Physiological Analysis

3.2.1. Oxalic Acid Content

The oxalic acid content in different treatments was analysed, and the results are presented in Figure 2. In the pathogen-inoculated treatment, the oxalic acid content was slightly higher than in the control. The treatment with the BCA showed a significantly lower oxalic acid content. When the preventive treatment was applied, the oxalic acid content increased to 7.22 nmol/g. Interestingly, the curative treatment exhibited a substantially higher oxalic acid content of 38.44 nmol/g.

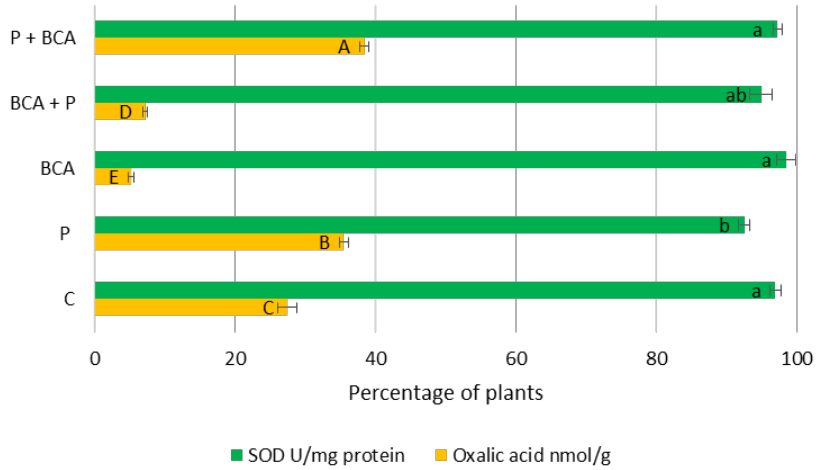

Figure 2. Oxalic Acid (nmol/g) and SOD (U/mg of protein) contents in *V. vinifera* plants in each treatment: control plants (C), plants inoculated with *M. guilliermondii* (BCA), and plants inoculated with *F. equiseti* (P), and those subjected to a dual inoculation; BCA + P, and P + BCA. Different letters accompanying the data in the figure denote statistically distinct groups ($p \leq 0.05$) via Duncan's test.

3.2.2. SOD Activity

The results of the experiment demonstrated variations in SOD activity among different treatment groups. The control group (C) exhibited a SOD activity of 96.96 U/mg of protein. In contrast, plants inoculated with the pathogen (P) showed a slightly lower SOD activity of 92.52 U/mg of protein. The treatment with the BCA led to a higher SOD activity of 98.48 U/mg of protein. Interestingly, the combined treatment of BCA and pathogen (BCA + P) resulted in a SOD activity of 94.93 U/mg of protein, which was lower than the BCA treatment alone. On the other hand, the treatment with pathogen + BCA (P + BCA) displayed a relatively higher SOD activity of 97.28 U/mg of protein. These findings suggest that the presence of BCA alone or in combination with the pathogen can influence the SOD activity in *V. vinifera* plants, indicating the potential modulation of the plant's antioxidant defence system in response to different treatments.

3.2.3. Salicylic Acid Content

Statistical analysis using the Duncan test revealed significant differences in the areas of salicylic acid production among the plants belonging to the BCA, Pathogen, and Control groups (** $p < 0.05$), emphasizing the distinct responses observed in each treatment. In the plants treated with the pathogen (*F. equiseti*), the average percentage of the affected area reached 1.34 ± 0.2%. The photos show small brown spots distributed throughout the leaf (Figure 3A). In the plants treated with yeast (BCA), the average percentage of the affected area in the observed leaves was 6.73 ± 1.7% (Figure 3B). Larger brown spots can be seen in these leaves compared to the control plants. In the leaves of the control plants (Figure 3C), brown spots corresponding to the formation of salicylic acid can be observed. The average percentage of affected area was found to be 2.76 ± 0.6%. In summary, the leaves from yeast-inoculated plants showed a higher affected leaf area, indicating the production of

salicylic acid. Conversely, the test group inoculated with *Fusarium equiseti* produced a lower percentage, approximately half the value obtained in the control plants.

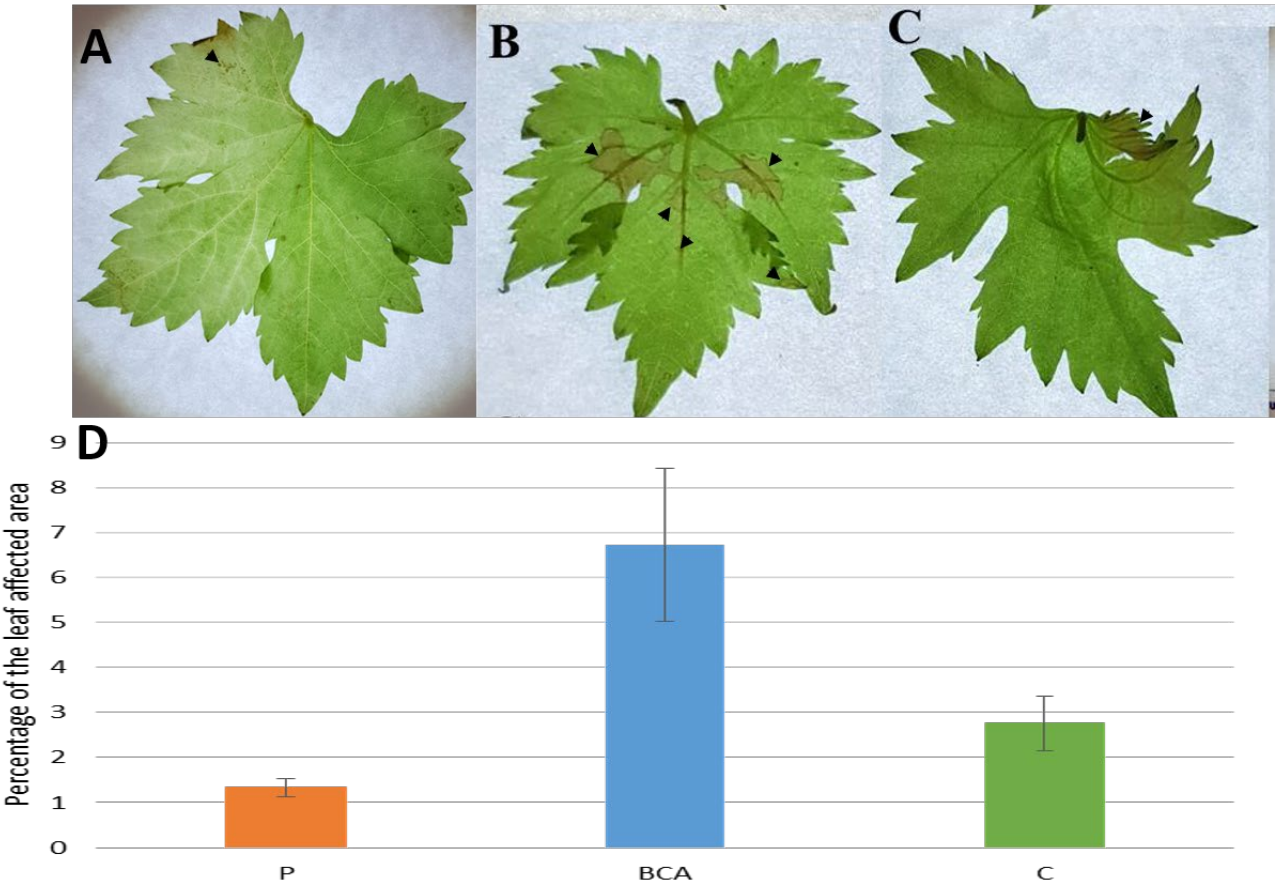

Figure 3. Photographic images for *V. vinifera* leaves with the presence of endogenous SA. (**A**) Plants inoculated with the pathogen *Fusarium equiseti*, P, exhibiting small brown spots distributed throughout the leaf, (**B**) Plants treated with yeast, BCA, displaying larger brown spots on the leaves, (**C**) Control plants, C, showing brown spots, indicating salicylic acid presence. Arrows indicate specific areas measured using ImageJ® software (Version 1.8.0) for quantitative analysis and the histogram (**D**) represents the quantitative analysis of salicylic acid area in the leaves for the plants from each treatment.

3.3. Differential Proteomics

We conducted a comprehensive analysis of differential proteomics across the different treatments. The main objective was to identify and characterize the protein expression changes induced by the BCA.

3.3.1. Identification of Differentially Expressed Proteins

Using state-of-the-art mass spectrometry and statistical analysis, we identified a total of 1463 unique proteins in the samples. Among these, 136 proteins were found to be differentially expressed across the four treatment groups (adjusted p-value < 0.05, fold change > 2). The heatmap of differentially expressed proteins is shown in Figure 4.

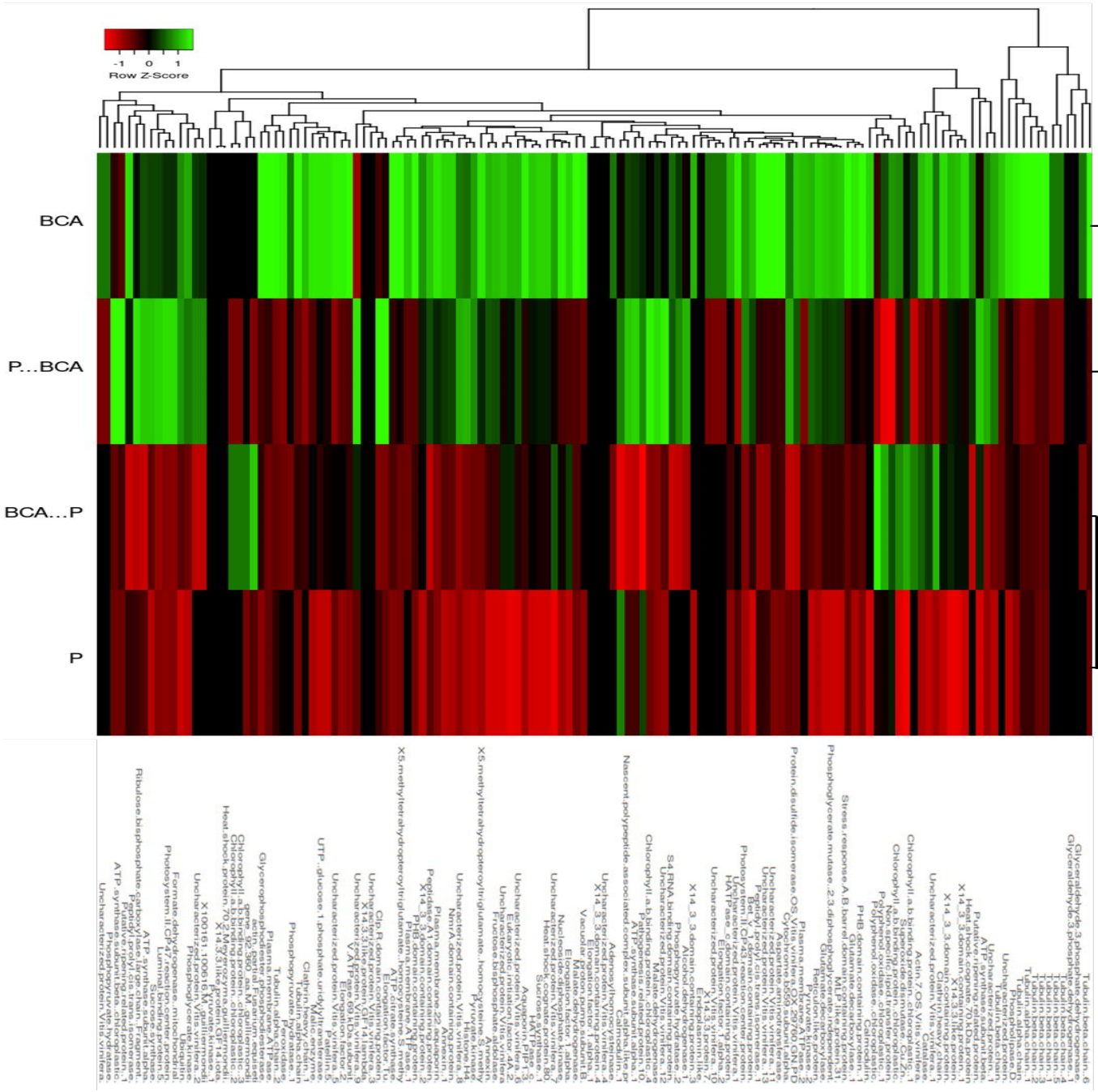

Figure 4. Heatmap of all treatments (BCA, P, BCA + P, and P + BCA). The green-to-red scale indicates low-to-high protein expression levels. Differentially expressed proteins were defined based on a threshold fold change > 2, at p-value < 0.05.

3.3.2. Functional Annotation and Pathway Analysis

To gain a deeper understanding of the biological implications of the differentially expressed proteins, we performed functional annotation and a pathway enrichment analysis. Notably, the differential proteomic analysis revealed significant enrichment in several biological processes affected by the treatments. The GO analysis highlighted the following important pathways and processes: microtubule cytoskeleton organization, the cellular response to unfolded protein, mitochondrial ATP synthesis-coupled proton transport, photosynthesis, light harvesting, glycolytic process, and receptor-mediated endocytosis (Figure 5).

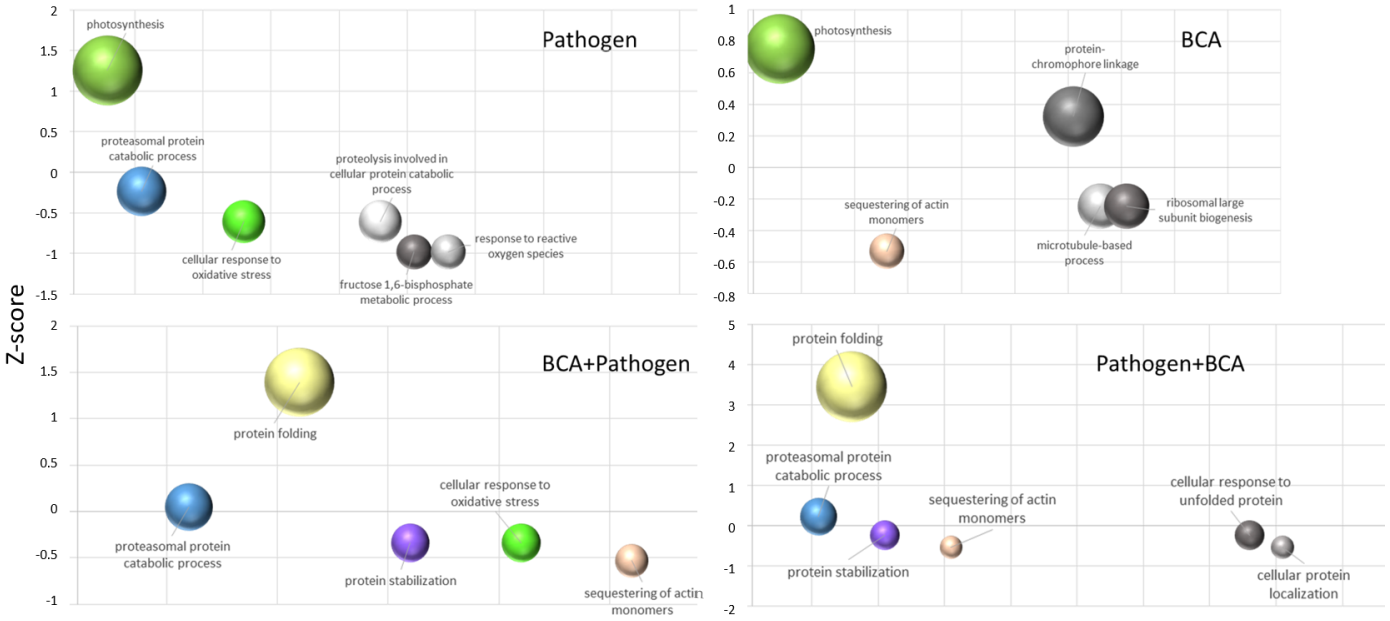

Figure 5. Top KEGG pathways enriched for the significantly differentially expressed proteins of all treatments (BCA, P, BCA + P, and P + BCA). Entries with larger bubbles contain more differential genes. The colour of the bubbles indicates a biological process. The smaller the enrichment *p*-value, the greater the degree of significance ($p < 0.05$).

3.3.3. Protein–Protein Interaction Network Analysis

In this study, we conducted a PPI network analysis to explore the potential interactions and functional relationships among the proteins of interest identified in the study. Using the data, we created a graphical representation of the PPI network. Each node in the network represents a protein, and the edges connecting the nodes indicate the interactions between the proteins (Figure 6). Furthermore, we focused on identifying putative key regulators or hub proteins that play central roles in the network.

In the case of the plants inoculated with the pathogen, there are two hub proteins related to the tubulin alpha chain and another one belonging to the actin family, highlighting the significance of the cytoskeleton in the plant–pathogen interaction.

For the plants inoculated with BCA, there are four hub proteins identified: tubulin alpha 2 chain, tubulin alpha 3 chain, and two heat shock proteins. In general, the identification of these hub proteins in the context of the BCA indicates that the cytoskeleton and heat shock proteins may be important components in the plant–BCA interaction.

For the plants with dual inoculation of BCA + P, there are diverse hub proteins: tubulin alpha chain and actin family proteins.

In the case of the plants inoculated with the dual P + BCA, we identified diverse hub proteins: tubulin, heat shock proteins, ubiquitin, and peptidyl-prolyl cis/trans isomerase. The presence of these hub proteins indicates that the combined treatment of P (pathogen) and BCA triggers responses that involve molecular chaperones and proteins associated with protein folding.

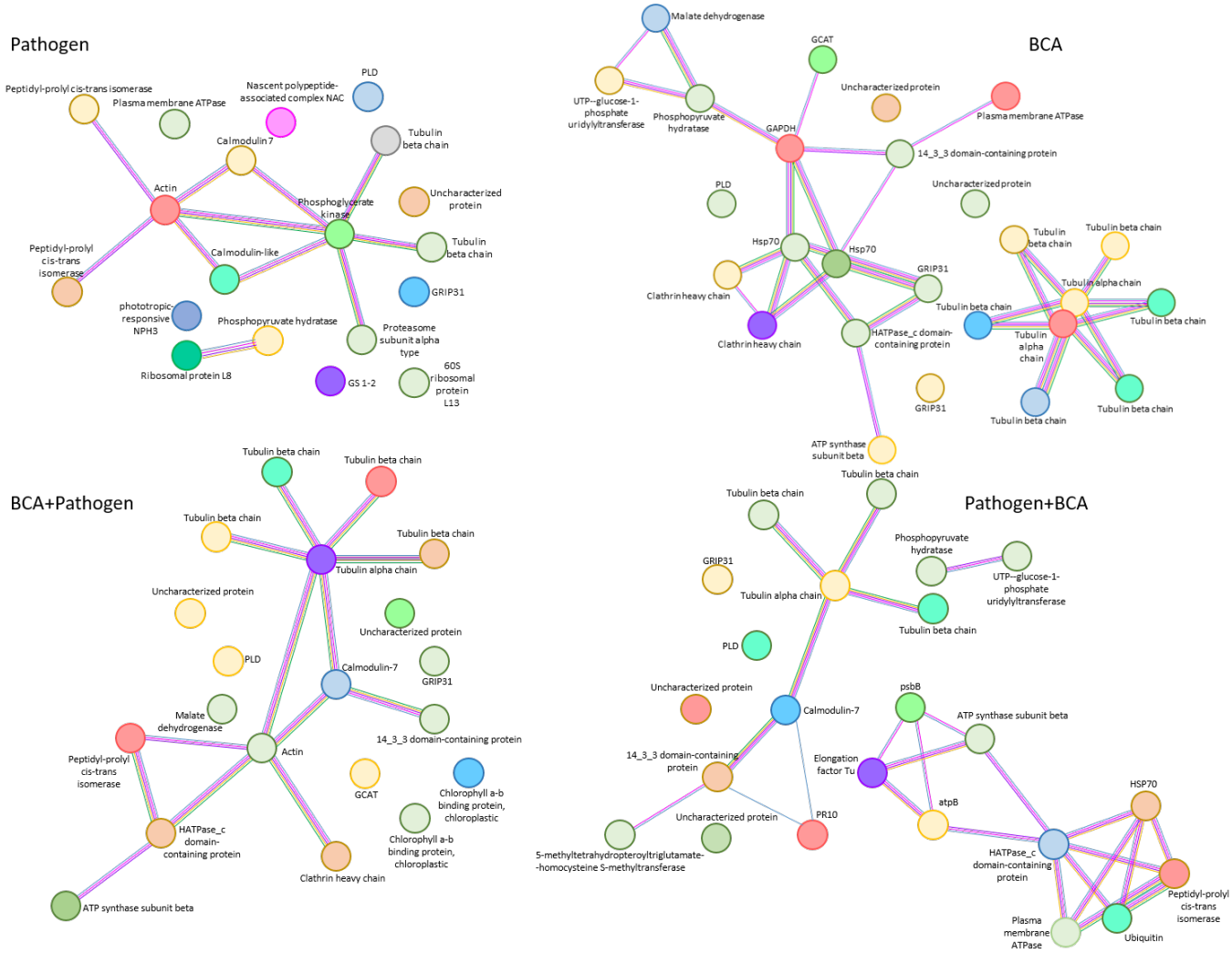

Figure 6. PPI network analysis of all treatments (BCA, P, BCA + P, and P + BCA). The PPI networks were constructed using the identified differentially expressed proteins from the differential proteomic analysis. Nodes represent individual proteins, while edges represent physical interactions between the proteins.

3.4. Gene Expression Patterns

The gene expression patterns of three differentially expressed PR genes were investigated under various treatments, including the BCA, P, BCA + P, and P + BCA. With respect to the proteins, thaumatin-like protein was detected exclusively in the P + BCA treatment. On the other hand, the other two proteins, β-1,3-glucosidase (also known as Beta-1,3-glucanase) and chitinase, were present in all treatments, but their accumulation was notably higher in the P + BCA treatment, followed by the BCA treatment (Figure 7a).

The RT-qPCR analysis highlights different patterns of regulation for the genes codifying the differentially expressed proteins in response to the various treatments. In the case of thaumatin and chitinase, the upregulation of *VviTL1* and *Vcchit1b* was observed in the samples treated with BCA and particularly in the treatment with the combined pathogen and BCA (Figure 7c,d). However, although *Vcgns1* also showed the highest levels of expression in these samples, the pattern was reversed, with the highest levels in the BCA-treated samples compared to P + BCA (Figure 7d).

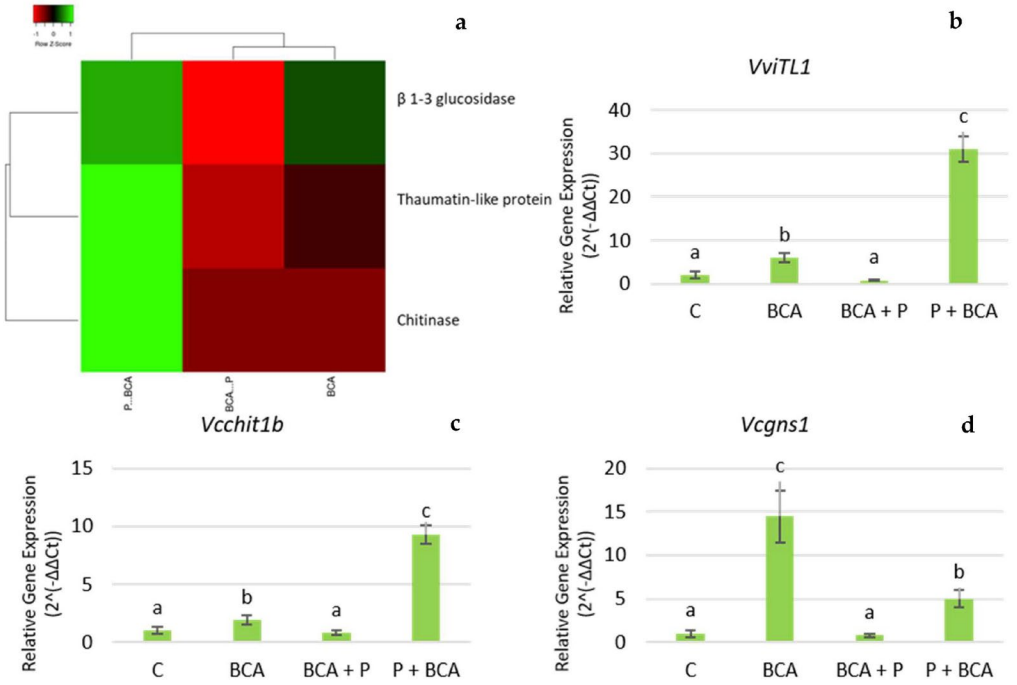

Figure 7. (**a**). Heatmap of three proteins (Beta 1–3 glucosidase, thaumatin-like protein, and chitinase) for the treatments including BCA inoculation (BCA, BCA + P, and P + BCA). The red-to-green scale indicates low-to-high protein expression levels. Differentially expressed proteins were defined based on a threshold fold change > 1.5, at $p < 0.05$. (**b**–**d**) Relative gene expression analysis of *VviTL1* (**b**), *Vcchit1b* (**c**), and *Vcgns1* (**d**) across different treatments (C, BCA, BCA + P, and P + BCA). Results were calculated relative to a calibrator sample (C) using the formula $2^{-\Delta\Delta Ct}$. Values are the mean ± SD, $n = 6$. Different letters accompanying the data in the figure denote statistically distinct groups ($p \leq 0.05$) via Duncan's test.

4. Discussion

Among the Fusarium species, *F. equiseti* has emerged as the causative agent, known to induce wilt diseases in a wide range of plant hosts, including grafted watermelon, grape, cucumber, tomato, cowpea, bean, and potato [14]. These findings highlight the significance of *F. equiseti* as a potential pathogen that poses a threat to various crops and underscores the need for effective disease management strategies to safeguard agricultural productivity.

The results of our experiment revealed distinct disease symptoms across different treatment groups (Figure 1). Vine plants inoculated with *F. equiseti* displayed significant disease symptoms, consistent with previous reports on the pathogenicity of this fungus [2]. On the other hand, the absence of disease symptoms in the yeast treatment group is in line with research highlighting the potential of BCAs, such as *M. guilliermondii*, to confer resistance against pathogens and promote plant health [15,16]. Additionally, our preventive treatment (BCA + P) exhibited a partial protective effect, while the curative treatment (P + BCA) demonstrated substantial disease suppression. These results suggest that treatment with the BCA *M. guilliermondii* (Patent CECT13190) induces enhanced defence responses in the host plant.

The ROS response is one of the early reactions that occur in plants when facing stress, and both oxalic acid and salicylic acid can be produced in response to the activation of these signalling pathways. The production of ROS can influence the synthesis and accumulation of salicylic acid and other defence metabolites. Salicylic acid acts as an antioxidant, directly scavenging reactive oxygen species and activating the plant's antioxidant defence systems. Additionally, oxalic acid may have effects on antioxidant enzymes, including superoxide dismutase (SOD).

Pathogen-inoculated plants displayed decreased salicylic acid content and SOD activity compared to control plants. This reduction in SOD activity aligns with previous findings indicating that pathogens can actively suppress antioxidant defences to facilitate their colonization and spread [17]. The decrease in SOD activity might disrupt the balance of ROS scavenging mechanisms, rendering the plant more susceptible to the oxidative stress and cell damage induced by the pathogen.

Conversely, the presence of the BCA led to a substantial increase in SOD activity in *V. vinifera* plants. This upregulation of SOD indicates the induction of an enhanced antioxidant defence response triggered by the BCA. BCAs are known to promote the synthesis of defence-related enzymes and secondary metabolites, contributing to the establishment of systemic resistance in plants [18]. The elevated SOD activity suggests that the BCA treatment is priming the plant's antioxidant defence system, protecting against oxidative stress induced by the pathogen.

In the combined treatment of BCA and pathogen, we observed intermediate SOD activity compared to the individual treatments. The combined treatment may trigger a complex defence mechanism, where the BCA primes the plant's antioxidant defence system while the pathogen attempts to suppress it.

Salicylic acid (SA) acts as a powerful phytohormone, influencing the generation of reactive oxygen species (ROS) and acting as a pro-oxidant, while also bolstering the activity of ROS-scavenging enzymes (like SOD) and serving as an antioxidant, particularly in stressful conditions. Intriguingly, the impact of SA on ROS dynamics in plants varies based on both time and concentration, with SA exhibiting the ability to augment ROS production (pro-oxidant) or facilitate ROS elimination (antioxidant), contingent upon these factors [19].

The salicylic acid content observed in our study is consistent with previous research demonstrating its involvement in plant defence responses [20]. The larger affected leaf area and salicylic acid production in yeast-treated plants aligns with the idea that BCAs can induce systemic acquired resistance (SAR) and activate the plant's immune response [21–23]. Conversely, the lower salicylic acid content in pathogen-inoculated plants might be attributed to pathogen suppression of host defence pathways, a common strategy employed by pathogens [24].

In our experiments, we have consistently observed a direct and consistent relationship between salicylic acid levels and superoxide dismutase (SOD) activity, specifically in treatments involving the biological control agent (BCA). Elevated salicylic acid levels positively correlate with a significant increase in SOD activity in our target plants under the influence of these yeast-based BCA treatments. In contrast, plants treated with the pathogen exhibit the opposite trend, correlating with increased disease symptoms. Lower salicylic acid concentrations coincide with more severe disease symptoms and a corresponding decrease in SOD activity.

In our study, we observed variations in oxalic acid content in response to different treatments, consistent with its dual role in plant defence mechanisms. At low concentrations, oxalic acid acts as a defence mechanism, but at high concentrations, it can become detrimental to plant health [25]. The pathogenic fungi of the genus *Fusarium*, known for producing high levels of oxalic acid, can cause damage to plant cells and inhibit the action of vital enzymes, ultimately benefiting the progression of the pathogen [26,27]. Pathogen-inoculated plants exhibited increased oxalic acid content, consistent with its role as a virulence factor facilitating infection. In contrast, plants treated with the BCA showed a reduction in oxalic acid content, suggesting the potential of the BCA to modulate the plant's biochemical response and limit the pathogen's virulence. Moreover, during the curative treatment involving both BCA and the pathogen, there was a significant increase in oxalic acid content, indicating a potential defence response elicited by this combined treatment.

The proteomic analysis of differentially expressed proteins across different treatments provides valuable insights into the complex molecular responses of *V. vinifera* plants to the biological control agent and pathogen interactions.

In the treatment involving only the pathogen (Figure 4), the overexpression of calmodulin and pathogenesis-related protein 10 (PR-10) signifies a focused activation of defence pathways aimed at countering the pathogen's attack [28,29]. The plant's intricate response to pathogenic challenges involves an interplay of biological processes (Figure 5). Pathogen exposure triggers a complex network of reactions, including the recalibration of photosynthesis and energy metabolism [30], enhanced protein turnover [31], and the management of oxidative stress [32]. In the presence of the pathogen, the hub proteins tubulin and actin (Figure 6) assume prominence. These proteins are central to cytoskeletal dynamics, and likely govern cellular responses to the pathogen involving cell structure and transport, and modulate processes like vesicle trafficking [33].

Our investigation into the differential protein expression profiles within the context of the biological control agent (BCA) interaction has revealed intriguing insights into the role of tubulins, key components of the cytoskeleton in mediating plant defence responses. Notably, our data indicate a distinct clustering of tubulin-related proteins in the dendrogram (Figure 4), showcasing their expression pattern in response to BCA inoculation. Upon exposure to BCA colonization, plants undergo microtubule network changes, influencing defence responses and cellular dynamics. Microtubule reorganization affects cell wall modifications, vesicle trafficking, and endocytosis, influencing defence compound secretion and nutrient uptake. Microtubules function as tracks for signalling molecule transport, affecting their distribution and the activation of defence genes. Tubulin dynamics impact phytohormone transport, influencing growth, development, and defence regulation. Altered microtubule organization affects phytohormone distribution, impacting root growth, stomatal closure, and defence gene induction. Moreover, microtubules potentially regulate exosome-mediated communication, impacting intercellular signalling via bioactive molecule exchange [34]. The application of the BCA treatment results in a wide range of effects on plant physiology, in particular on several key biological processes. Among these, photosynthesis occupies a central position. Additionally, protein-chromophore linkage influences protein function and signalling pathways [35]. Ribosomal large subunit biogenesis enhances protein synthesis mechanisms. The treatment also involves sequestering actin monomers, potentially indicating cytoskeletal adjustments. The presence of hub proteins (Figure 6) corresponding to heat shock proteins suggests that the BCA may trigger stress responses in the plant [36], and these chaperone proteins could be involved in protecting and stabilizing key proteins. Meanwhile, tubulin signifies a potential modulation of cellular dynamics in response to the BCA. Tubulin's involvement implies the role of BCA in cellular organization, transport, and signalling. Further exploration of the molecular mechanisms linking tubulins, cytoskeletal dynamics, and exosome-mediated communication holds promise for advancing our understanding of the plant defence strategies modulated by this BCA.

The differential expression of specific proteins in the BCA + pathogen treatment (Figure 4) underscores a sophisticated interplay of responses aimed at mitigating the detrimental effects of pathogen invasion while potentially harnessing the benefits of the application of the biological control agent. The induction of catalase and superoxide dismutase points towards a concerted effort to counteract the oxidative stress generated during the pathogen attack. Increased expression of these antioxidant enzymes suggests the activation of defence mechanisms to neutralize harmful reactive oxygen species and maintain cellular redox balance [37]. The detection of chlorophyll a b-binding protein and polyphenol oxidase indicates a potential optimization of photosynthetic processes and regulation of phenolic compounds. This response could signify an effort to sustain energy production and enhance phenolic defences against the pathogen [38], respectively. The upregulation of actin 7 may signify dynamic cytoskeletal rearrangements essential for defence responses and pathogen recognition. Actin dynamics play a pivotal role in orchestrating cellular processes such as vesicle trafficking, cell wall modifications, and signal transduction, contributing to effective defence mechanisms [39]. Protein folding and proteasomal protein catabolism emphasize the plant's commitment to maintaining

proper protein conformation and quality control. The cellular response to unfolded protein underscores a direct reaction to proteotoxic stress, indicating a tightly regulated mechanism to handle misfolded proteins. Protein stabilization stands as a parallel strategy, ensuring the durability of essential proteins. The sequestering of actin monomers hints at cytoskeletal modifications that might play a role in orchestrating these responses. In the context of the BCA + pathogen treatment, the hub proteins are the tubulin alpha chain and an actin family protein (Figure 6). The tubulin alpha chain likely modulates cytoskeletal dynamics, and the actin family protein signifies roles in cytoskeleton rearrangements and signalling cascades. The presence of the tubulin alpha chain as a hub protein suggests its potential involvement in coordinating cellular responses during the interaction between the plant, the biological control agent, and the pathogen [40]. Changes in the cytoskeleton dynamics may be essential for the plant's defence responses and adaptations to the presence of both the biological control agent and the pathogen. However, to firmly establish the functional significance of these observations, further research is warranted. Future studies will be essential to confirm and elaborate on the implications of cytoskeleton modifications in coordinating cellular responses during the interaction between the plant, the BCA, and the pathogen.

The observed upregulation of specific proteins in response to the pathogen + BCA treatment (Figure 4) suggests a coordinated and complex cellular response aimed at defence and adaptation. The induction of alcohol dehydrogenase, phosphopyruvate hydratase, and malate dehydrogenase likely reflects metabolic adjustments to enhance energy production and metabolic fluxes under stress conditions [41]. The increased expression of pathogenesis-related proteins and the S4 RNA binding domain indicates an activated defence response against the pathogen. This heightened expression of defence-related proteins suggests a robust attempt by the plant to counteract the invading pathogen while potentially triggering downstream signalling cascades. The induction of calmodulin and elongation factor may signify the activation of calcium-dependent signalling pathways [42] and translation machinery, respectively, both of which play integral roles in coordinating stress responses and protein synthesis. The elevated expression of a nascent polypeptide-associated complex and Clp R domain could imply enhanced protein folding, quality control, and proteolysis, reflecting the cellular machinery's response to stress-induced protein damage and the need to manage misfolded proteins [43]. Furthermore, the presence of putative ripening protein and histone H4 could hint at complex regulatory mechanisms orchestrating developmental [44] and epigenetic responses under stress conditions. Notably, processes such as cellular protein localization and proteasomal protein catabolic activity underscore the regulation of protein homeostasis. The interplay between protein folding and stabilization points to the plant's effort to maintain protein structure and function under stress conditions (Figure 5). The cellular response to oxidative stress is a key element in the defence mechanisms. Additionally, the sequestering of actin monomers suggests an active restructuring of the cytoskeleton. The hub proteins for this dual inoculation treatment (Figure 6), collectively underscore the complex interplay between cytoskeletal dynamics, signalling [45], protein stability, folding, and turnover [46] in shaping the plant's adaptive response. These mechanisms are likely to be part of the plant's defence strategy against the pathogen, aiding in the proper folding and functioning of proteins essential for defence responses and resistance against pathogens.

The efficacy of the P + BCA treatment demonstrated a favourable association with the upregulation of defence-related genes, namely β-1,3-glucanase, thaumatin, and chitinase. This alignment of transcriptomic and proteomic domains further reinforces the empirical robustness of the results.

β-1,3-glucosidases, also called β-1,3-glucanases, are hydrolytic enzymes capable of inducing phytohormonal signals and triggering the release of antimicrobial secondary metabolites through glycosyl residue removal. This enzymatic activity enables swift plant responses to pathogenic intrusion and facilitates activation of the SA pathway [47]. Additionally, the application of *M. guilliermondii* not only heightened β-1,3-glucosidase activity

but also that of chitinase, underscoring the potential of this beneficial microorganism to reinforce host defence mechanisms [48,49]. β-1,3-glucosidase and chitinase are vital when a plant is under attack from fungi. Plant chitinases are strongly expressed when plant cells are under pathogen stress, playing a critical role against fungal pathogens. Chitinases are induced in plants in response to either a biocontrol agent or a plant pathogen [50].

The upregulation of the gene codifying a thaumatin-like protein, as inferred from the transcriptional analysis, corresponds with the previously established augmented abundance of this protein in the proteomic analysis on the P + BCA treatment. This similarity between transcriptomic and proteomic findings lends substantial corroboration to the key role ascribed to the thaumatin-like protein within the plant's defence, particularly in its coordinated responsiveness to the dual stimuli posed by pathogen and BCA. The multifunctional attributes of this protein in plant defence mechanisms have been extensively documented [51,52], including diverse roles such as pathogen recognition, antimicrobial activity, and the modulation of stress-induced signalling pathways in the plant.

Thaumatin-like proteins, with antifungal capabilities, can disrupt target membranes and possess the potential to bind and hydrolyse fungal β-1,3-glucans [53]. β-1,3-glucans are carbohydrate-derived molecular motifs recognized by plants, initiating immune responses and bolstering disease resistance [54].

5. Conclusions

In conclusion, our investigation delves deep into the oxidative stress pathway managed by antioxidant enzymes like SOD, coupled with dynamic shifts in metabolites such as oxalic acid and salicylic acid, to drive the plant's defensive responses. This study shows the interplay of cellular dynamics, cytoskeletal adjustments, and proteomic reconfigurations in *V. vinifera* due to the interaction between the biological control agent *M. guilliermondii* (Patent CECT13190) and the pathogen *F. equiseti*. These comprehensive findings not only enrich our understanding of the modulation in the plant's defences but also offer promising avenues for pioneering viticulture strategies. These findings collectively enhance our comprehensive understanding of the modulation of the plant's defences, offering promising avenues for innovative and sustainable agricultural practices that harness biocontrol agents to generate a more robust and eco-friendly approach to crop protection.

Author Contributions: Conceptualization, A.G.-G. and B.P.L.; methodology, A.G.-G. and M.T.S.-B.; investigation, J.M.A.d.R. and N.O.P.; resources, A.G.-G. and M.T.S.-B.; data curation, M.L.T.M.; writing—original draft preparation, J.M.A.d.R. and A.G.-G.; writing—review and editing, A.G.-G., M.L.T.M. and M.T.S.-B.; supervision, A.G.-G. and B.P.L.; project administration, A.G.-G.; funding acquisition, A.G.-G. All authors have read and agreed to the published version of the manuscript.

Funding: This research was funded by the Instituto Nacional de Investigación y Tecnología Agraria y Alimentaria (INIA-CSIC), Madrid, Spain (RTA2015-0015-C02-02 Project).

Data Availability Statement: No new data were created or analyzed in this study. Data sharing is not applicable to this article.

Acknowledgments: The authors would like to express their gratitude to Raquel Alonso Valenzuela who contributed to the successful completion of this research. We extend our sincere thanks to the INIA-CSIC for their financial support, which made this study possible. The proteomic analysis was performed in the Proteomics Unit of Complutense University of Madrid, which belongs to ProteoRed, PRB3-ISCIII, supported by grant PT17/0019 of the PE I+D+i 2013–2016, and funded by ISCIII and ERDF.

Conflicts of Interest: The authors declare no conflict of interest.

References

1. Gramaje, D.; Armengol, J. Fungal trunk pathogens in the grapevine propagation process: Potential inoculum sources. *Plant Dis.* **2011**, *95*, 1040–1044. [CrossRef]
2. Astudillo-Calderón, S.; Tello, M.L.; Alonso de Robador, J.M.; Pintos, B.; Gómez-Garay, A. First Report of *Fusarium equiseti* Causing Vascular Wilt Disease on *Vitis vinifera* in Spain. *Plant Dis.* **2019**, *103*, 2471. [CrossRef]

3. Morsy, E.A.; Osman, A.K.; Taha, N.R.; Ibrahim, H.A. Improvement of growth and some metabolic activities in faba bean plants (*Vicia faba* L.) by using the yeast *Meyerozyma guilliermondii* in saline-sodic soil. *Environ. Sci. Pollut. Res.* **2020**, *27*, 33872–33885.
4. Yang, Q.; Zhang, X.; Solairaj, D.; Fu, Y.; Zhang, H. Molecular Response of *Meyerozyma guilliermondii* to Patulin: Transcriptomic-Based Analysis. *J. Fungi* **2023**, *9*, 538. [CrossRef]
5. Aguirre-Güitrón, L.; Calderón-Santoyo, M.; Bautista-Rosales, P.U.; Ragazzo-Sánchez, J.A. Application of powder formulation of *Meyerozyma caribbica* for postharvest control of *Colletotrichum gloeosporioides* in mango (*Mangifera indica* L.). *LWT* **2019**, *113*, 108271. [CrossRef]
6. Arnold, A.E.; Mejía, L.C.; Kyllo, D.; Rojas, E.I.; Maynard, Z.; Robbins, N.; Herre, E.A. Fungal endophytes limit pathogen damage in a tropical tree. *Proc. Natl. Acad. Sci. USA* **2003**, *100*, 15649–15654. [CrossRef]
7. Hoagland, D.R.; Arnon, D.I. The water-culture method for growing plants without soil. *Circ. Calif. Agric. Exp. Stn.* **1950**, *347*, 1–32.
8. Baggiolini, M. Sur la biologie de quelques champignons parasites de la vigne. *Ann. L'institut Natl. Rech. Agron.* **1952**, *2*, 1–44.
9. Sherman, B.T.; Hao, M.; Qiu, J.; Jiao, X.; Baseler, M.W.; Lane, H.C.; Imamichi, T.; Chang, W. DAVID: A web server for functional enrichment analysis and functional annotation of gene lists (2021 update). *Nucleic Acids Res.* **2022**, *50*, W216–W221. [CrossRef] [PubMed]
10. Tseng, C.Y.; Hung, Y.C.; Hu, Y.C.; Tseng, Y.T.; Chen, C.T.; Chen, Y.J.; Lee, S.R. The effects of titania nanotubes with embedded TiO2 nanoparticles on the attachment and growth of keratinocytes and fibroblasts. *Biomaterials* **2014**, *35*, 603–612.
11. Romero, I.; Vazquez-Hernandez, M.; Escribano, M.I.; Merodio, C.; Sanchez-Ballesta, M.T. Expression profiles and DNA-binding affinity of five ERF genes in bunches of *Vitis vinifera* cv. Cardinal treated with high levels of CO_2 at low temperature. *Front. Plant Sci.* **2016**, *7*, 1748. [CrossRef] [PubMed]
12. Romero, I.; Alegria, E.; Gonzalez de Pradena, A.; Vazquez-Hernandez, M.; Escribano, M.I.; Merodio, C.; Sanchez-Ballesta, M.T. WRKY transcription factors in the response of table grapes (cv. Autumn Royal) to high CO_2 levels and low temperature. *Postharvest Biol. Technol.* **2019**, *150*, 42–51. [CrossRef]
13. Livak, K.J.; Schmittgen, T.D. Analysis of relative gene expression data using real-time quantitative PCR and the $2^{-\Delta\Delta CT}$ method. *Methods* **2001**, *25*, 402–408. [CrossRef] [PubMed]
14. El-Morsy, E.S.M.; Elmalahy, Y.S.; Mousa, M. Biocontrol of *Fusarium equiseti* using chitosan nanoparticles combined with *Trichoderma longibrachiatum* and *Penicillium polonicum*. *Fungal Biol. Biotechnol.* **2023**, *10*, 5. [CrossRef]
15. Papon, N.; Savini, V.; Lanoue, A.; Simkin, A.J.; Crèche, J.; Giglioli-Guivarc'h, N.; Clastre, M.; Courdavault, V.; Sibirny, A.A. *Candida guilliermondii*: Biotechnological applications, perspectives for biological control, emerging clinical importance and recent advances in genetics. *Curr. Genet.* **2013**, *59*, 73–90. [CrossRef]
16. Kthiri, Z.; Jabeur, M.B.; Chairi, F.; López-Cristoffanini, C.; López-Carbonell, M.; Serret, M.D.; Araus, J.L.; Karmous, C.; Hamada, W. Exploring the potential of *Meyerozyma guilliermondii* on physiological performances and defense response against Fusarium crown rot on durum wheat. *Pathogens* **2021**, *10*, 52. [CrossRef]
17. Saleem, M.; Fariduddin, Q.; Castroverde, C.D.M. Salicylic acid: A key regulator of redox signalling and plant immunity. *Plant Physiol. Biochem.* **2021**, *168*, 381–397. [CrossRef]
18. Kużniak, E.; Skłodowska, M. Fungal pathogen-induced changes in the antioxidant systems of leaf peroxisomes from infected tomato plants. *Planta* **2005**, *222*, 192–200. [CrossRef]
19. Ankati, S.; Srinivas, V.; Pratyusha, S.; Gopalakrishnan, S. Streptomyces consortia-mediated plant defense against Fusarium wilt and plant growth-promotion in chickpea. *Microb. Pathog.* **2021**, *157*, 104961. [CrossRef]
20. Loake, G.; Grant, M. Salicylic acid in plant defense—The players and protagonists. *Curr. Opin. Plant Biol.* **2007**, *10*, 466–472. [CrossRef]
21. Edgar, C.I.; McGrath, K.C.; Dombrecht, B.; Manners, J.M.; Maclean, D.C.; Schenk, P.M.; Kazan, K. Salicylic acid mediates resistance to the vascular wilt pathogen *Fusarium oxysporum* in the model host *Arabidopsis thaliana*. *Australas. Plant Pathol.* **2006**, *35*, 581–591. [CrossRef]
22. Moya-Elizondo, E.A.; Jacobsen, B.J. Integrated management of Fusarium crown rot of wheat using fungicide seed treatment, cultivar resistance, and induction of systemic acquired resistance (SAR). *Biol. Control.* **2016**, *92*, 153–163. [CrossRef]
23. Lahlali, R.; Ezrari, S.; Radouane, N.; Kenfaoui, J.; Esmaeel, Q.; El Hamss, H.; Belabess, Z.; Barka, E.A. Biological control of plant pathogens: A global perspective. *Microorganisms* **2022**, *10*, 596. [CrossRef] [PubMed]
24. Patkar, R.N.; Naqvi, N.I. Fungal manipulation of hormone-regulated plant defense. *PLoS Pathog.* **2017**, *13*, e1006334. [CrossRef]
25. Kim, K.S.; Min, J.Y.; Dickman, M.B.; Mamo, B.E.; Eriksen, R.L.; Adhikari, N.D.; Hayes, R.J.; Mou, B.; Simko, I.; You, J.; et al. Oxalic acid is an elicitor of plant programmed cell death during *Sclerotinia sclerotiorum* disease development. *Mol. Plant-Microbe Interact.* **2008**, *21*, 605–612. [CrossRef]
26. De la Torre, M.A.; Gomez-Alarcon, G.; Melgarejo, P.; Sáiz-Jiménez, C. Fungi in weathered sandstone from Salamanca cathedral, Spain. *Sci. Total Environ.* **1991**, *107*, 159–168. [CrossRef]
27. Gómez-Alarcón, G.; Munoz, M.L.; Flores, M. Excretion of organic acids by fungal strains isolated from decayed sandstone. *Int. Biodeterior. Biodegrad.* **1994**, *34*, 169–180. [CrossRef]
28. Santos Lopes, N.; Silva Santos, A.; Pereira Silva de Novaes, D.; Pirovani, C.P.; Micheli, F. Pathogenesis-related protein 10 (PR-10) in resistance to biotic stress: Progress in elucidating functions, regulation, and modes of action. *Front. Plant Sci.* **2022**, *14*, 1193873. [CrossRef]

29. Wanford, J.J.; Odendall, C. Ca^{2+}-calmodulin signalling at the host-pathogen interface. *Curr. Opin. Microbiol.* **2023**, *72*, 102267. [CrossRef]
30. Berger, S.; Sinha, A.K.; Roitsch, T. Plant physiology meets phytopathology: Plant primary metabolism and plant–pathogen interactions. *J. Exp. Bot.* **2007**, *58*, 4019–4026. [CrossRef]
31. Raffeiner, M.; Zhu, S.; González-Fuente, M.; Üstün, S. Interplay between autophagy and proteasome during protein turnover. *Trends Plant Sci.* **2023**, *28*, 698–714. [CrossRef] [PubMed]
32. Tyagi, S.; Shah, A.; Karthik, K.; Rathinam, M.; Rai, V.; Chaudhary, N.; Sreevathsa, R. Reactive oxygen species in plants: An invincible fulcrum for biotic stress mitigation. *Appl. Microbiol. Biotechnol.* **2022**, *106*, 5945–5955. [CrossRef] [PubMed]
33. Wang, J.; Lian, N.; Zhang, Y.; Man, Y.; Chen, L.; Yang, H.; Lin, J.; Jing, Y. The cytoskeleton in plant immunity: Dynamics, regulation, and function. *Int. J. Mol. Sci.* **2022**, *23*, 15553. [CrossRef] [PubMed]
34. Li, S.; Cao, P.; Wang, C.; Guo, J.; Zang, Y.; Wu, K.; Ran, F.; Liu, L.; Wang, D.; Min, Y. Genome-wide analysis of the tubulin gene family in cassava and expression of family member FtsZ2-1 during various stress. *Plants* **2021**, *10*, 668. [CrossRef] [PubMed]
35. Sazegari, S.; Zinati, Z.; Tahmasebi, A. Dynamic transcriptomic analysis uncovers key genes and mechanisms involved in seed priming-induced tolerance to drought in barley. *Gene Rep.* **2020**, *21*, 100941. [CrossRef]
36. Sahu, P.K.; Jayalakshmi, K.; Tilgam, J.; Gupta, A.; Nagaraju, Y.; Kumar, A.; Hamid, S.; Singh, H.V.; Minkina, T.; Rajput, V.D.; et al. ROS generated from biotic stress: Effects on plants and alleviation by endophytic microbes. *Front. Plant Sci.* **2022**, *13*, 1042936. [CrossRef]
37. Haider, M.S.; Jaskani, M.J.; Fang, J. Overproduction of ROS: Underlying molecular mechanism of scavenging and redox signaling. In *Biocontrol Agents and Secondary Metabolites*; Woodhead Publishing: Sawston, UK, 2021; pp. 347–382.
38. Panina, Y.; Fravel, D.R.; Baker, C.J.; Shcherbakova, L.A. Biocontrol and plant pathogenic *Fusarium oxysporum*-induced changes in phenolic compounds in tomato leaves and roots. *J. Phytopathol.* **2007**, *155*, 475–481. [CrossRef]
39. Hückelhoven, R. Cell wall–associated mechanisms of disease resistance and susceptibility. *Annu. Rev. Phytopathol.* **2007**, *45*, 101–127. [CrossRef]
40. Marathe, R.; Dinesh-Kumar, S.P. Plant defense: One post, multiple guards?! *Mol. Cell* **2003**, *11*, 284–286. [CrossRef]
41. Cobos, R.; Barreiro, C.; Mateos, R.M.; Coque, J.J.R. Cytoplasmic- and extracellular-proteome analysis of *Diplodia seriata*: A phytopathogenic fungus involved in grapevine decline. *Proteome Sci.* **2010**, *8*, 46. [CrossRef]
42. Yadav, M.; Pandey, J.; Chakraborty, A.; Hassan, M.I.; Kundu, J.K.; Roy, A.; Singh, I.K.; Singh, A. A comprehensive analysis of calmodulin-like proteins of glycine max indicates their role in calcium signaling and plant defense against insect attack. *Front. Plant Sci.* **2022**, *13*, 817950. [CrossRef]
43. Leidhold, C.; Voos, W. Chaperones and proteases—Guardians of protein integrity in eukaryotic organelles. *Ann. N. Y. Acad. Sci.* **2007**, *1113*, 72–86. [CrossRef] [PubMed]
44. Yang, L.; Lin, H.; Takahashi, Y.; Chen, F.; Walker, M.A.; Civerolo, E.L. Proteomic analysis of grapevine stem in response to *Xylella fastidiosa* inoculation. *Physiol. Mol. Plant Pathol.* **2011**, *75*, 90–99. [CrossRef]
45. Alvarez, M.E.; Savouré, A.; Szabados, L. Proline metabolism as a regulatory hub. *Trends Plant Sci.* **2022**, *27*, 39–55. [CrossRef]
46. Sharma, S.; Prasad, A.; Prasad, M. Ubiquitination: A perspective from plant pathogens. *J. Exp. Bot.* **2023**, *74*, 4367–4376. [CrossRef] [PubMed]
47. Morant, A.V.; Jørgensen, K.; Jørgensen, C.; Paquette, S.M.; Sánchez-Pérez, R.; Møller, B.L.; Bak, S. β-Glucosidases as detonators of plant chemical defense. *Phytochemistry* **2008**, *69*, 1795–1813. [CrossRef] [PubMed]
48. Madhupani, Y.D.S.; Adikaram, N.K.B. Delayed incidence of stem-end rot and enhanced defenses in *Aureobasidium pullulans*-treated avocado (*Persea americana* Mill.) fruit. *J. Plant Dis. Prot.* **2017**, *124*, 227–234. [CrossRef]
49. de Jong, H.; Reglinski, T.; Elmer, P.A.; Wurms, K.; Vanneste, J.L.; Guo, L.F.; Alavi, M. Integrated use of *Aureobasidium pullulans* strain CG163 and acibenzolar-S-methyl for management of bacterial canker in kiwifruit. *Plants* **2019**, *8*, 287. [CrossRef] [PubMed]
50. Vaghela, B.; Vashi, R.; Rajput, K.; Joshi, R. Plant chitinases and their role in plant defense: A comprehensive review. *Enzym. Microb. Technol.* **2022**, *159*, 110055. [CrossRef]
51. Vigers, A.J.; Wiedemann, S.; Roberts, W.K.; Legrand, M.; Selitrennikoff, C.P.; Fritig, B. Thaumatin-like pathogenesis-related proteins are antifungal. *Plant Sci.* **1992**, *83*, 155–161. [CrossRef]
52. Liu, J.J.; Sturrock, R.; Ekramoddoullah, A.K. The superfamily of thaumatin-like proteins: Its origin, evolution, and expression towards biological function. *Plant Cell Rep.* **2010**, *29*, 419–436. [CrossRef] [PubMed]
53. Grenier, J.; Potvin, C.; Trudel, J.; Asselin, A. Some thaumatin-like proteins hydrolyze polymeric β-1, 3-glucans. *Plant J.* **1999**, *19*, 473–480. [CrossRef] [PubMed]
54. Rebaque, D.; Del Hierro, I.; Lopez, G.; Bacete, L.; Vilaplana, F.; Dallabernardina, P.; Pfrengle, F.; Jordá, L.; Sánchez-Vallet, A.; Pérez, R.; et al. Cell wall-derived mixed-linked β-1, 3/1, 4-glucans trigger immune responses and disease resistance in plants. *Plant J.* **2021**, *106*, 601–615. [CrossRef] [PubMed]